RESEARCH PAPER

Dynamic changes of metabolomics and expression of candicidin biosynthesis gene cluster caused by the presence of a pleiotropic regulator AdpA in *Streptomyces* ZYJ-6

Xiaoyun Liu[1] · Xiaojuan Sun[1] · Weimin He[1] · Xiwei Tian[1] · Yingping Zhuang[1] · Ju Chu[1]

Abstract

Candicidin is one of the frequent antibiotics for its high antifungal activity, but the productivity is still extremely low. Introduction of *adpA* into *Streptomyces* ZYJ-6 could improve candicidin productivity significantly and achieved 9338 µg/mL, which was the highest value ever reported in the literature. Combined analyses of transcriptional levels, metabolic flux and metabolomics indicate that *para*-aminobenzoic acid and the first step of shikimic acid metabolism were not the bottleneck for the candicidin production in the control. However, methylmalonyl-CoA played a central role in the candicidin production and the gene *methB* responsible for the biosynthesis of methylmalonyl-CoA might be the candidate gene target for further improving the production of candicidin.

Keywords Metabolomics · qRT-PCR · FBA · Candicidin · *Streptomyces*

Introduction

Candicidin, which was produced by *Streptomyces griseus* from the cow manure [1], is one of the heptaenes macrolide antifungal antibiotics. Candicidin was named due to its high antifungal activity against *Candida albicans* [2]. Coincidently, a novel antibiotic of FR-008 was described to kill *Saccharomyces cerevisiae* [3] and, subsequently, it was verified that the candicidin and the FR-008 were the identical compounds in *Streptomyces griseus* and *Streptomyces* FR-008, respectively [4].

The candicidin/FR-008 production has become a major interest for both scientific research and industrial application. However, the highest titer of the candicidin was 4000 µg/mL [5]. *Streptomyces* ZYJ-6 was originated from *Streptomyces*

✉ Ju Chu
juchu@ecust.edu.cn

1   State Key Laboratory of Bioreactor Engineering, School of Biochemical Engineering, East China University of Science and Technology, Room 413, Building 18, Shanghai 200237, People's Republic of China

FR-008 with the combined inactivation of KR21 and DH18 and it could produce the most effective component of FR-008-III with a C-3 ketone and a C-9 hydroxyl, and the titer was 450 µg/mL [6]. In our previous work, the titer of the FR-008 can reach 5161 µg/mL in *Streptomyces* ZYJ-6 based on the medium and process optimization (Liu et al. 2018).

AdpA is a central transcriptional regulator in the A-factor regulatory cascade. A-factor, as a microbial hormone, was first identified in *S. griseus* by Khokhlov et al. [7]. A-factor at a certain level would bind to the A-factor receptor protein (ArpA) and change the conformation of ArpA leading to the ArpA dissociation from the DNA. ArpA bound the *adpA* promoter so that the transcription of *adpA* was switched on. AdpA then activated a number of the genes, which was related to the mycelium formation and antibiotic biosynthesis [8].

Specifically, AdpA was able to bind the promoter of *strR*, a regulatory gene involved in the transcription of streptomycin biosynthetic genes in *S. griseus*. It was found that the disruption of *adpA* would result in the cease of streptomycin biosynthesis and the overexpression of *adpA* would lead to the significant enhancement of streptomycin production in the wild-type *S. griseus* strain [9]. Six AdpA-dependent genes involving in primary or secondary metabolism were identified and their expression was directly activated by this pleiotropic regulator AdpA in *Streptomyces lividans* [10].

High transcriptional levels of *adpA-H* (the *Streptomyces hygroscopicus* ortholog of *adpA*) and validamycin biosynthetic genes made the validamycin production increase by 55% [11]. *Streptomyces avermitilis* also contains an ortholog of *adpA* (*adpA-a*) and no difference was found in avermectin production between the *adpA-a* mutant and the wild-type strain. However, *adpA-a* was involved in the regulation of the melanin production and the morphological differentiation [12]. The mutation of *adpA* in *Streptomyces coelicolor* caused bald colonies and reduction of the actinorhodin, suggesting that AdpA in *S. coelicolor* (designated as AdpA SC) also played an important role in the regulation of both morphological differentiation and secondary metabolism [13].

In summary, *adpA* could transcriptionally multi-regulate the genes of morphological differentiation and secondary metabolism. An alignment of the AdpA sequences from *Streptomyces* FR-008 and *Streptomyces coelicolor* showed an ortholog similarity of about 87%, inferring that *adpA* from *S. coelicolor* might also function and enhance antibiotic candicidin production in *Streptomyces* FR-008-derived strain *Streptomyces* ZYJ-6. The *adpA* gene from *S. coelicolor* was cloned into the integrating plasmid pIB139 with PermE* to give pFAdpA. This plasmid was integrated into the genome of strain *Streptomyces* ZYJ-6 by conjugation and named *Streptomyces* ZYJ-6 pFAdpA [14]. In this study, *Streptomyces* ZYJ-6 was taken as the control and the performance of *Streptomyces* ZYJ-6 pFAdpA (mutant) was compared through the analyses of the macroscopic metabolism, the metabolomics, flux balance analysis (FBA) and the transcriptional analysis of candicidin biosynthesis gene cluster.

Methods and materials

Microorganism and cell growth conditions

Streptomyces ZYJ-6 and *Streptomyces* ZYJ-6 pFAdpA mutant were kindly donated by professor Delin You in Shanghai Jiao Tong University, China.

Spores were prepared by the slant culture on SFM medium (2% agar, 2% mannitol, 2% soybean powder, pH 7.2) for 4 days at 30 °C. A 500-mL Erlenmeyer flask with 100 mL TSBY medium (3% TSB, 1% yeast extract, 10.3% sucrose, pH 7.2) was inoculated with 10^7 spores and then cultivated for 30 h at 30 °C and 220 rpm. 300 mL mycelia suspension was inoculated in a 5-L fermenter for candicidin fermentation.

The fed-batch fermentation culture was carried out in a 5-L (3-L starting volume) turbine-stirred bioreactor (Shanghai Guoqiang Bioengineering Equipment Co., Ltd. Shanghai, China). The chemically defined medium contained (1/L) glucose 55 g, KH_2PO_4 1.5 g, $(NH_4)_2SO_4$ 1.8 g, EDTANa$_2$ 1.8 g, $MgSO_4 \cdot 7H_2O$ 8.6 g, $ZnSO_4 \cdot 7H_2O$ 35.7 mg, $CaCl_2$ 50 mg, $FeSO_4 \cdot 7H_2O$ 28.7 mg, $CuSO_4 \cdot 5H_2O$ 42 mg, $MnSO_4 \cdot H_2O$ 9.1 mg, antifoam 0.3%, NaCl 9.0 g as an osmotic pressure regulator. The pH of the process was controlled at 6.8–7.8 by adding 10% ammonium hydroxide solution (Liu et al. 2018). The bioreactor with medium was sterilized at 121 °C for 60 min. The agitation, temperature, aeration and overpressure were set at constant levels of 400 rpm, 30 °C, 1 vvm and 0.05 MPa, respectively. The feeding was initiated once the initial glucose was depleted and then the residual glucose concentration was controlled below 5 g/L. The glucose concentration in the feeding solution was 428 g/L and it was sterilized separately at 110 °C for 40 min.

Samples for macroscopic metabolism analysis

Regular sampling (per 12 h) contained 3×3 mL culture which was used for dry cell weight (DCW) measurement. Briefly, 3 mL culture was deposited on the pre-weighed filter paper and washed thrice with the distilled water. The filter paper with the cells was dried to constant weight in a 70 °C oven for 36 h and cooled to room temperature in a desiccator and then the filter paper was weighed and the biomass was calculated. One milliliter culture was centrifuged, and the supernatant was used for the determination of residual glucose concentration. The glucose concentration was determined by a biosensor (SBA-40B, Shandong Science Academy, China). One milliliter culture was taken in 2 mL dimethylsulfoxide (DMSO) directly for FR-008-III/candicidin D extraction and the mixed solution was subjected to ultra-sonication for 30 min. After the centrifugation, the extracted solution was filtered readily for HPLC injection for the quantification of candicidin. The candicidin was measured according to the procedures as described by Mao et al. [15]. Briefly, the column was SB-C$_{18}$ from Agilent and the temperature was kept at 25 °C. The mobile phase was 40% acetonitrile and 60% 5 mM NH$_4$Ac (pH = 4.5) with isocratic elution and the flow rate was 0.6 mL/min. The detection wavelength was 380 nm.

Samples for metabolomics study

The samples for metabolomic analyses were withdrawn at 36 h, 46 h, 96 h and 156 h, respectively, which represented the time point in the exponential phase, in the initial synthesis phase, in the high production phase of candicidin and in the late phase, respectively. About 1 mL culture was withdrawn into 8 mL isoamylol:base solution = 5:1 (v/v) and base solution was acetone:ethanol = 1:1 (mol/mol) by rapid sampling device within 0.2 s. The mixed solution was centrifuged for 1 min at − 13 °C and 7500 rpm and the supernatant was discarded. Adding internal standard (IS), the residual cell pellets were suspended in 50% (v/v) methanol and then

subjected to three cycles of freezing in liquid nitrogen for 3 min and thawing at −30 °C on cryostat. After the supernatant was centrifuged and filtered, the extracted solution was concentrated to 0.5 g for metabolomic detection by GC–MS and UPLC–MS/MS.

Quantitative analysis of amino acids, phosphate sugars, organic acids and sugar alcohols was carried out by GC–MS (Agilent, Santa Clara, CA, USA). The optimized determination conditions were referred to Jonge et al. [16] with some minor modifications in the column and temperature gradients. Briefly, the flow velocity of helium was set as 1 mL/min during the analysis. 1 μL sample was injected into HP5-5% Phenyl Methicone column (30 m × 250 μm internal diameter, 0.25 μm film thickness) with a splitless mode at 250 °C for injection. The GC column temperature for the amino acid analysis was incipiently set as 100 °C for 1 min and then increased with a speed of 10 °C/min up to 300 °C and held 10 min at 300 °C, while for the metabolites of the phosphate sugars, organic acids and sugar alcohols, the incipient temperature was set as 70 °C for 1 min and then raised up by the speed of 10 °C/min up to 300 °C and held 10 min at 300 °C. Electron ionization was always operated with 70 eV and the temperatures of transfer line, MS source and quadrupole were set as 280 °C, 230 °C and 150 °C as described before by Jonge et al. [16]. The quantification of targeted metabolites was conducted by isotope dilution mass spectrometry (IDMS) in selected ion monitoring (SIM) mode [17].

The coenzymes were analyzed by ultrahigh-performance liquid chromatography–mass spectrometry/tandem isotope dilution mass spectrometry (UHPLC–MS/IDMS) (Thermal Ultimate 3000 UPLC system coupling to a Thermal TSQ Quantum Ultra mass spectrum system) as described by Hong et al. [18].

Quantitative real-time polymerase chain reaction (qRT-PCR)

The sampling time for qRT-PCR was set at 36 h, 46 h, 96 h and 156 h, respectively. Two milliliter culture was withdrawn into a 10-mL tube and then frozen into the liquid nitrogen immediately and stored at −80 °C until the RNA extraction. Axygen® AxyPrep™ Multisource RNA Midiprep Kit was used for the total RNA extraction and PrimeScriptTM RT reagent Kit with gDNA Eraser (Perfect Real Time) for cDNA synthesis, following procedures recommended by the manufacturers.

Quantitative Real Time PCR (qRT-PCR) was performed in Bio-Rad CFX96 Real-Time PCR Detection System using SYBR® Premix Ex Taq™ GC (Perfect Real Time) and the following protocol: 30 s at 95 °C (initial template denaturation), 39 cycles at 95 °C for 5 s (denaturation) and 60 °C for 30 s (primer annealing); melting curve 65–95 °C and increment 0.5 °C for 5 s. Samples were taken in triplicate, and each sample was run in triplicate.

The expression levels of target genes were normalized using *hrdB* gene as endogenous control and the abundance of *hrdB* gene did not vary under our experimental conditions [19]. The critical threshold cycle (C_T) was defined for each sample. The fold changes in the transcript levels were calculated using the following equations: $\Delta C_T = C_T$ (target gene) − C_T (reference gene), $\Delta\Delta C_T = \Delta C_T$ (treatment) − ΔC_T (control), and the ratio = $2^{-\Delta\Delta CT}$ [20]. All primers used and the annotated functions of genes in this study are listed in Table 1.

Data processing

The calibration curve for the intracellular metabolites was established by IDMS method. The raw data from GC–IDMS and UHPLC–MS/IDMS were converted to concentration data by Chemstation in Agilent and Xcalibur in ThermoFisher, respectively. The unit of the intracellular metabolite concentration was converted into μmol per g dry cell weight. The statistical analysis was realized by the software of *R* language.

Metabolic flux analysis

The model of metabolic flux analysis was referenced from Chen et al. [21]. The consumption rates of glucose, oxygen and ammonium hydroxide as well as the production rates of candicidin and carbon dioxide were involved in the metabolic flux analysis. The metabolic fluxes were calculated by MATLAB. The reactions list and the stoichiometry coefficient matrix could be found in Tables S1 and S2, respectively.

Results and discussion

Comparison of the macroscopic metabolism in *Streptomyces* ZYJ-6 and *Streptomyces* ZYJ-6 pFAdpA mutant

Physiological profiles of *Streptomyces* ZYJ-6 (control) and *Streptomyces* ZYJ-6 pFAdpA (mutant) are shown in Fig. 1. Except for the introduction of *adpA* in the mutant, other conditions were kept the same for the two strains, but their fermentation performances and kinetic parameters were obviously different (Fig. 1 and Table 2).

Surprisingly, the titer of candicidin reached 9338 μg/mL in the mutant, which was the highest level in the literature ever reported and 1.8 times of 5161 μg/mL from the control (Fig. 1a). Interestingly, the onset of candicidin biosynthesis was at 40 h in the mutant, which was 4 h earlier

Table 1 Sequences of primers for quantitative real-time polymerase chain reaction (qRT-PCR) and annotated functions of genes

Number	Genes and primers	Sequence 5′–3′	Annotated functions
1	*pabAB*-F	CTTCTCGTCGACAACTACGA	Biosynthesis of starter unit PABA
	pabAB-R	GAGAGCACCACGTTGTCGAA	
2	*pabC*-F	CTCACCAACTACGGCCATTT	Biosynthesis of starter unit PABA
	pabC-R	GTCGAAGACGGTGACACGGA	
3	*fscA*-F	ATGAGGCGGAACAGCTCCTC	Type I PKS loading module and module 1
	fscA-R	AGTTGGAGGCGCTGCTCGTCT	
4	*fscB*-F	TGAAGGCGGATTCCTCCACGA	Type I PKS modules 2–4
	fscB-R	ACGAAGACACCGGTGGTGCT	
5	*fscC*-F	ATGGCAAGCTCCGAAGCCAA	Type I PKS modules 5–10
	fscC-R	AACCGGCAGGCCATGCCGAT	
6	*fscD*-F	ATGGACAAGGAACAGAAGC	Type I PKS modules 11–16
	fscD-R	AGCATCTTCCACAGGTCCTC	
7	*fscE*-F	AAGTTGTCGAAGCTCTCCGG	Type I PKS modules 17–20
	fscE-R	ACGAGGTGCCACAGGTCCT	
8	*fscF*-F	ATGACAAGAAGCTCGTCGAC	Type I PKS modules 21 + TE
	fscF-R	AGGAGCCGCCAGTACTCCT	
9	*fscR3*-F	TGGTGACGGTGACCGGAGAA	Transcriptional regulator regulation
	fscR3-R	TGCTCGTCGGTGAGGAAGA	
10	*fscR4*-F	AATCGGCAAGACCGCACTGCT	Transcriptional regulator regulation
	fscR4-R	TCAGGCCGAGTCCGCCGAACA	
11	*fscM2*-F	CCGGTGATGTACTCCTGGT	Mycosamine biosynthesis
	fscM2-R	TGTTCTTCAAGCCGATGAG	
12	*fscM3*-F	ATGTCCAAGCGTGCACTCAT	Mycosamine biosynthesis
	fscM3-R	AGCTTGGCGATCCGGTCCTT	
13	*fscTE*-F	ATCTCCGTGTTGACCGCGT	Type II thioesterase removal of aberrant intermediates
	fscTE-R	CATCGAGACCTACACCTG	
14	*skaK*-F	TTGGAGAGTTCTGTGATGGT	Biosynthesis of shikimic acid
	skaK-R	CGAGGTCGAACTCATCTGCT	
15	*methB*-F	TCATGCGTGCTTCAACTCCA	Biosynthesis of methylmalonyl-CoA
	methB-R	AGTGGCGCGAACTGATGGA	
16	*adpA*-F	GCCACCACGCACTGGATGTA	Pleiotropic regulator
	adpA-R	ACGATGTGCAGGCACAGGTC	
17	*hrdB*-F	GCGGTGGAGAAGTTCGACTACA	Reference gene
	hrdB-R	AGCTTGTTGATGACCTCGACCAT	

than that in the control. Moreover, compared to the candicidin average synthesis rate (q_P) of 22.48 mg/g.h in the control, the q_P in the mutant was significantly enhanced to 64.27 mg/g.h (Table 2). However, the tendencies of glucose consumption were almost coincident in the two strains and the glucose average consumption rate (q_S) also presented same values (Table 2). On the other hand, the cell growth shown in Fig. 1c displayed distinct difference between the two strains. The highest biomass and the maximum specific growth rate (μ_{max}) of the mutant achieved were 25.15 gDCW/kg and 0.078 1/h, respectively; in contrast, they were only 15.08 gDCW/kg and 0.064 1/h in the control. These results indicated that the mutant seemed to be beneficial in supporting cell growth (Fig. 1a). Simultaneously, the

mutant had few impacts on the glucose utilization, while it could significantly improve the yield of candicidin based on glucose (Ysp) (Table 2). Additionally, through the oxygen uptake rate (OUR) profile (Fig. 1d), which was an important physiological parameter to represent cell activity, it could be observed that although curves were almost coincident in the earlier stage of two strains, the discrepancy appeared after 100 h which might be ascribed to the production of the candicidin (Fig. 1c).

The *adpA* was a gene involved in the morphological differentiation and secondary metabolism [22]. It was deduced that the *adpA* would regulate the cell growth and candicidin biosynthesis. As expected, under same culture condition, the mutant was favorable to enhancing the
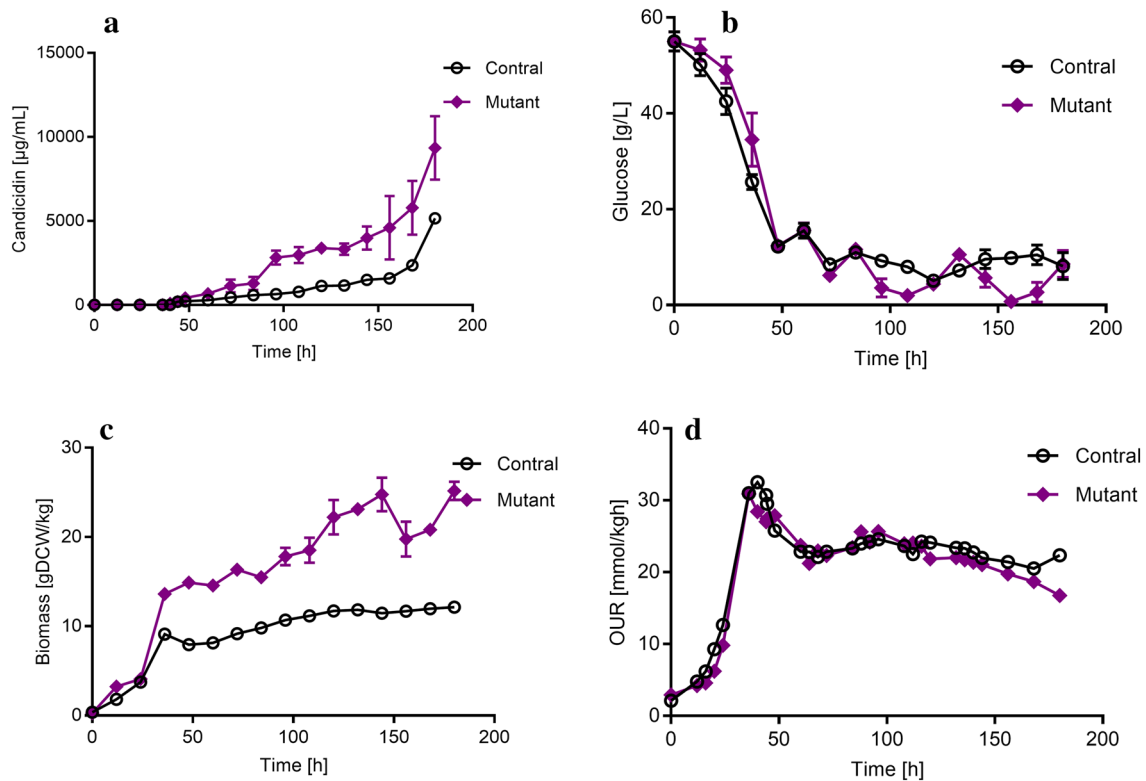
Fig. 1 Physiological profiles of the control (*Streptomyces* ZYJ-6, hollow circle) and the mutant (*Streptomyces* ZYJ-6 pFAdpA, solid diamond) in fed-batch cultivations. The parameters including candicidin **a**, glucose **b**, biomass **c** and OUR (oxygen uptake rate, **d**). All the parameters were measured based on at least triplicate measurements. The sudden increase of glucose concentration in **b** represents the pulsed addition of glucose

Table 2 Kinetic parameters for the control (*Streptomyces* ZYJ-6) and the mutant (*Streptomyces* ZYJ-6 pFAdpA)

Terms	μ_{max}	q_S	q_P	q_O	Ysp	Yxp	Yop
[−]	[1/h]	[g/g.h]	[mg/g.h]	[mmol/g.h]	[mg/g]	[mg/g]	[mg/mmol]
Control	0.064 ± 0.004	0.31 ± 0.028	22.48 ± 1.53	3.25 ± 0.26	72.52 ± 5.32	702.5 ± 26.47	6.92 ± 0.39
Mutant	0.078 ± 0.004	0.31 ± 0.031	64.27 ± 5.11	2.41 ± 0.19	207.32 ± 15.24	1647.95 ± 60.01	26.67 ± 1.34

μ_{max} the maximum specific growth rate, q_S glucose average consumption rate, the unit is g glucose per g biomass per hour, q_P candicidin average synthesis rate, the unit is mg candicidin per g biomass per hour, q_O oxygen average consumption rate, the unit is mmol oxygen per g biomass per hour, Ysp the yield of candicidin based on glucose, equal to q_P/q_S, the unit is mg candicidin per g glucose, Yxp the yield of candicidin based on biomass, equal to q_P/μ, the unit is mg candicidin per g biomass; Yop the yield of candicidin based on oxygen, equal to q_P/q_O, the unit is mg candicidin per mmol oxygen

candicidin production and beneficial to supporting cell growth. However, it was difficult to understand the potential mechanism only through macroscopic analyses. To this end, the changes of the intracellular metabolomics, the expression of genes involved in candicidin biosynthesis and the metabolic flux distributions were investigated to unravel the influencing mechanism of the *adpA*.

Comparison of the intracellular metabolomics in the control and mutant

The metabolites from the control and mutant with different capabilities of candicidin production were analyzed by a combination of GC–IDMS and UHPLC–MS/IDMS. A total of 39 intracellular metabolites were identified and quantified

Table 3 Intracellular metabolites concentration in the control and mutant at different time points: 36, 46, 96 and 156 h

Metabolites	36 h		46 h		96 h		156 h	
	Control	Mutant	Control	Mutant	Control	Mutant	Control	Mutant
Precursors								
Shikimate	0.22±0.02	0.45±0.05	0.74±0.12	1.54±0.25	0.85±0.02	1.24±0.07	0.09±0.01	0.70±0.00
PABA	1.63±0.20	2.08±0.02	7.31±0.41	5.90±0.95	6.40±0.43	7.10±0.08	6.39±0.42	6.58±0.37
CoA	0.16±0.02	0.42±0.04	0.15±0.02	0.48±0.12	0.10±0.03	0.39±0.07	0.21±0.02	0.49±0.09
Malonyl-CoA	4.92±1.10	4.56±0.85	0.71±0.12	4.34±1.29	0.62±0.05	26.42±11.15	29.8±6.37	57.48±7.82
Methylmalonyl-CoA	3.06±0.74	0.05±0.01	0.04±0.01	0.04±0.00	0.07±0.01	4.87±1.37	23.63±1.37	24.12±0.16
Acetyl-CoA	1.52±0.25	0.61±0.08	0.10±0.02	0.46±0.02	0.31±0.03	4.37±0.69	1.84±0.28	1.46±0.27
Propionyl-CoA	0.97±0.15	0.51±0.14	0.02±0.00	0.40±0.01	0.04±0.00	20.52±3.23	0.6±0.09	19.38±3.10
Amino acid metabolism								
Alanine	51.24±3.71	46.04±9.76	11.06±2.01	102.63±30.52	165.89±33.24	365.95±15.93	169.87±24.28	376.59±25.13
Glycine	2.55±0.15	1.74±0.29	0.75±0.17	2.87±0.68	6.08±0.63	6.48±0.49	4.22±0.56	6.18±0.07
Valine	6.27±0.47	1.77±0.18	0.93±0.14	1.98±0.36	11.15±2.36	26.44±1.88	6.22±0.87	33.74±0.77
Leucine	5.42±0.23	0.55±0.07	1.21±0.14	0.86±0.24	6.54±1.29	2.91±0.31	3.56±0.49	7.80±0.30
Isoleucine	1.25±0.15	0.28±0.01	0.30±0.05	0.33±0.05	2.31±0.38	3.42±0.44	1.72±0.20	6.92±0.21
Proline	2.05±0.17	0.56±0.08	0.40±0.08	0.54±0.02	2.38±0.54	16.18±1.09	1.82±0.30	13.27±0.22
Methionine	1.09±0.04	0.25±0.03	0.76±0.08	0.51±0.06	1.09±0.15	2.05±0.21	0.80±0.16	2.14±0.19
Serine	2.78±0.18	0.59±0.10	0.81±0.17	0.87±0.09	5.25±1.11	8.60±0.69	3.79±0.6	5.86±0.06
Threonine	3.42±0.24	1.92±0.43	0.77±0.16	2.49±0.20	13.37±0.12	49.10±3.19	10.08±1.47	53.57±0.38
Phenylalanine	4.9±0.19	0.93±0.18	4.33±0.42	1.53±0.02	5.41±0.75	2.00±0.54	4.19±0.64	1.40±0.16
Aspartate	7.24±0.23	4.34±0.94	3.45±0.84	5.36±0.50	3.97±1.25	7.23±0.52	5.82±1.02	10.28±0.46
Glutamate	154.83±18.24	637.44±19.83	36.14±6.75	254.44±60.14	65.07±16.42	789.88±34.26	139.27±22.98	174.15±3.69
Ornithine	1.01±0.15	0.77±0.17	0.46±0.07	0.77±0.11	0.62±0.07	2.00±0.39	0.73±0.07	1.29±0.21
Asparagine	0.88±0.12	0.41±0.11	0.59±0.19	0.89±0.10	4.69±0.95	3.49±0.21	3.59±0.42	4.69±0.63
Glutamine	18.09±0.74	17.52±4.8	4.28±1.11	23.08±3.45	12.65±3.06	119.72±6.77	25.19±4.38	38.74±1.59
Tyrosine	1.7±0.32	0.13±0.01	0.57±0.09	0.35±0.05	0.99±0.11	0.28±0.06	0.46±0.06	1.59±0.34
Central carbon metabolism								
Pyruvate	0.61±0.01	1.94±0.13	0.75±0.10	1.99±0.26	0.62±0.04	0.67±0.06	0.59±0.00	0.78±0.02
Succinate	0.61±0.04	0.55±0.08	0.23±0.06	0.92±0.07	0.39±0.10	1.84±0.47	0.57±0.11	0.03±0.01
Fumarate	0.19±0.01	0.32±0.03	0.16±0.03	0.38±0.06	0.18±0.03	0.32±0.05	0.18±0.04	0.26±0.01
Malate	0.20±0.04	0.66±0.16	0.15±0.04	1.11±0.30	0.16±0.04	0.55±0.05	0.27±0.03	0.29±0.03
α-Ketoglutarate	0.14±0.01	1.33±0.36	0.11±0.01	1.92±0.21	0.12±0.00	2.32±0.16	0.08±0.01	0.74±0.06
Citrate	3.62±0.46	0.28±0.01	5.66±0.09	0.84±0.22	2.26±0.02	0.98±0.04	4.67±0.07	1.80±0.03
Ribose 5-phosphate	1.28±0.11	1.08±0.19	3.75±0.85	1.02±0.29	1.07±0.24	1.38±0.06	0.74±0.01	1.20±0.27
Glyceraldehyde 3-phosphate	14.83±1.71	0.25±0.03	18.33±1.2	0.19±0.04	8.44±1.02	0.27±0.03	14.75±1.24	0.26±0.03
6-Phosphogluconate	0.75±0.02	0.55±0.03	5.08±0.84	1.01±0.09	3.03±0.39	1.71±0.14	1.09±0.13	1.49±0.06
Sedoheptulose 7-phosphate	3.39±0.47	0.85±0.05	1.42±0.30	1.28±0.27	1.37±0.19	3.41±0.22	22.55±1.44	4.12±0.02
3-Phosphoglycerate	2.90±0.44	0.79±0.02	2.43±0.10	0.91±0.04	2.68±0.24	1.38±0.11	2.42±0.29	0.79±0.02
Fructose 6-phosphate	2.80±0.12	1.15±0.25	4.58±0.47	1.78±0.31	3.16±0.48	1.88±0.12	2.20±0.31	1.84±0.01
Glucose 6-phosphate	12.52±0.66	4.81±0.88	22.19±3.42	7.18±1.62	12.22±1.79	3.72±0.26	9.36±1.64	8.10±0.10
Sugar alcohols								
Erythritol	1.87±0.08	0.95±0.13	3.09±0.42	1.45±0.16	1.91±0.17	1.27±0.18	1.70±0.20	2.23±0.63
Xylitol	0.18±0.01	0.13±0.00	0.32±0.07	0.24±0.03	0.19±0.04	0.39±0.11	0.25±0.02	0.34±0.03
Arabitol	0.66±0.15	0.37±0.01	0.29±0.08	1.47±0.24	1.69±0.03	1.81±0.40	0.24±0.04	0.15±0.01

The values represent the means of three independent experiments and the error bars represent standard deviations of three values. The unit was μmol/gDCW

by standards, including amino acids from the amino acids metabolism, organic acids and phosphate sugars from the central carbon metabolism, coenzymes from the precursors and sugar alcohols (Table 3).

First, the quality of data was assessed by the heatmap combining with the cluster analysis (CA) (Fig. 2a). The metabolites from the control (C1–C4) and mutant (M1–M4) were separated into two groups clearly indicating the discrepancy between the control and mutant was statistically significant. Interestingly, aspartate (Asp), methionine (Met), isoleucine (Ile), threonine (Thr), valine (Val), alanine (Ala), and proline (Pro) were assigned to one subgroup with the candicidin and would be discussed in more detail later. After that, the principal component analysis (PCA) (Fig. 2b) reconfirmed the statistical significance between the control and mutant. The four time points in the control (red) were separated clearly from those in the mutant (green). On the basis of these results from the CA and PCA, it was reasonable to conclude that the intracellular metabolite data of the control and mutant were statistically significant and suitable for further analyses.

Moreover, by the partial least squares (PLS) analysis, the variable importance of the projection (VIP) was gained. The higher the VIP score, the closer the candicidin biosynthesis. Total of 14 metabolites closely associated with the candicidin production were selected (VIP score > 1) for further discussion (Fig. 2c). They were Ile, Ala, Thr, Val, Asp, glycine (Gly), asparagine (Asn), Propionyl-CoA, Met, Pro, serine (Ser), xylitol (Xyl), leucine (Leu) and para-aminobenzoic acid (PABA). Most of them belong to amino acids and precursors. Subsequently, the metabolites highly correlating with the candicidin biosynthesis were classified into different categories and mapped onto the metabolic pathways (Fig. 3).

Amino acids were important not only in supporting cell growth but also for polyketide precursors [23]. There were 12 amino acids out of 14 metabolites, which were closely associated with the candicidin biosynthesis by PLS, i.e., Ile [VIP score = 1.75], Ala [VIP score = 1.71], Thr [VIP score = 1.63], Val [VIP score = 1.63], Asp [VIP score = 1.51], Gly [VIP score = 1.48], Asn [VIP score = 1.48], Met [VIP score = 1.43], Pro [VIP score = 1.40], Ser [VIP score = 1.26], Leu [VIP score = 1.10], and PABA [VIP score = 1.08] (Fig. 2c).

Ile, Thr, Asp, Asn and Met belong to the Asp family generated from the oxaloacetate (Oxa) in TCA. Clearly, the above five amino acids had significant uptrend in the mutant (Table 3). Before 46 h (growth period), the levels were lower, but after 46 h (production period), their levels were increased rapidly and kept higher levels till 156 h. The concentrations of Ile and Thr were 3.42 μmol/gDCW and 49.1 μmol/gDCW, respectively, at 96 h, which were almost 10 times and 20 times higher than those at 46 h (0.33 μmol/

gDCW and 2.49 μmol/gDCW) (Table 3). Transitional period (from 46–96 h) was the key period for the cell growth and candicidin production (Fig. 1a, c). Notably, in the control, the concentrations of these five amino acids were lowest at 46 h, at which time the candicidin began to synthesize. After 46 h, the levels of these five amino acids fluctuated and reached the highest level at 96 h but still lower than those of the mutant. The amino acids from Asp family were the direct sources of Propionyl-CoA biosynthesis [VIP score = 1.45] (Fig. 2c) and Propionyl-CoA could be further converted to methylmalonyl-CoA which was one of the direct precursors for the candicidin biosynthesis. Thus, it was speculated that the supply of precursors was the main reason for significant difference between the control and mutant on the candicidin biosynthesis.

Ala, Val and Leu belong to the pyruvate (Pyr) family generated from Pyr in EMP. Surprisingly, the above three amino acids had the same uptrend with the five amino acids from the Asp family in the mutant. And the concentrations of these three amino acids were also lowest at 46 h and then fluctuated and reached the highest levels at 96 h in the control (Table 3). The concentration of Val was 1.98 μmol/gDCW at 46 h and 26.44 μmol/gDCW at 96 h, which increased by 13.35 times. As same to the amino acids from Asp family, Val was also the direct source for Propionyl-CoA biosynthesis. Therefore, the amino acids from Pyr family might play a similar role to supply precursors for the candicidin biosynthesis as that of Asp family.

Although Gly, Pro, Ser and PABA belong to different families, they performed same trends. Before 46 h (growth period), the levels were lower, but after 46 h (production period), their levels were increased rapidly and kept higher till 156 h (except for PABA). It was suggested that Gly, Pro and Ser were beneficial for the production of candicidin. PABA was the starter unit for candicidin production but its concentrations were very close between the control and mutant (Table 3), indicating that PABA seemed not the limiting factor for candicidin production in the control.

Additionally, Ala, Gly, Ser and Thr could be converted to AceCoA by Pyr; Asp and Asn could be converted to Oxa; Leu could be converted to AceCoA by acetoacetyl-CoA and Pro could be converted to αKG by glutamate (Glu). All these metabolites could enter into TCA to supply energy for the candicidin biosynthesis and cell growth. Met, Ile and Val could be converted to succinyl-CoA (SucCoA) which is isomeride of Methylmalonyl-CoA and could be transformed to Methylmalonyl-CoA easily.

As a result, although the control and mutant were cultivated under the same condition, the adpA caused different pool sizes of precursor amino acids and brought big differences in the candicidin biosynthesis. Amino acids were crucial not only for the cell growth but also for the secondary metabolism. In summary, the amino acids from

a

b

c
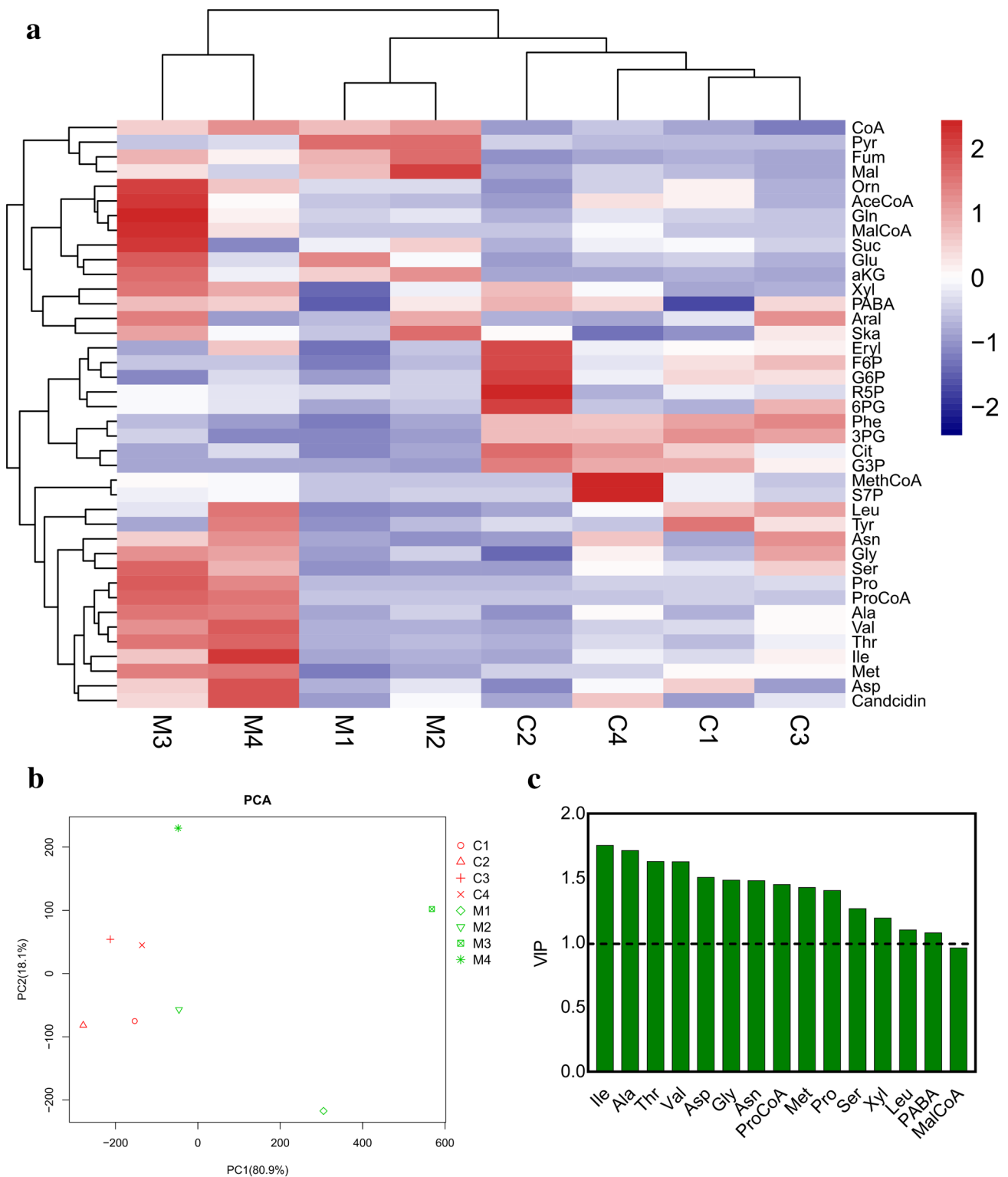
Asp and Pyr families were insufficient in the control leading to the low levels of intracellular Propionyl-CoA and Methylmalonyl-CoA which subsequently resulted in slower candicidin production rate during 46–96 h, compared to the mutant. Indeed, the concentrations of Propionyl-CoA and

Methylmalonyl-CoA (Fig. 3 and Table 3) further proved the above assumption. Particularly, at 96 h, the concentrations of Propionyl-CoA and Methylmalonyl-CoA were 0.04 and 0.07 μmol/gDCW in the control, whereas those were 20.52 and 4.87 μmol/gDCW in the mutant, which were 513 and 70

◀**Fig. 2** Cluster analysis, PCA and PLS (VIP) of intracellular metabolites from the control (C1–C4) and mutant (M1–M4). Samples were rapidly withdrawn from the cultivations at 36, 46, 96, and 156 h. **a** Cluster-derived heatmap; **b** PCA-derived score plots; **c** PLS-derived the variable importance of the projection (VIP) histogram. C1/M1 was the first time points of the control or mutant. Pyr, pyruvate; Fum, fumarate; Mal, malate; Orn, ornithine; AceCoA, acetyl-CoA; Gln, glutamine; MalCoA, malonyl-CoA; Suc, succinate; Glu, glutamate; αKG, α-ketoglutarate; Xyl, xylitol; PABA, *para*-aminobenzoic acid; Aral, arabitol; Ska, shikimic acid; Eryl, erythritol; F6P, fructose 6-phosphate; G6P, glucose 6-phosphate; R5P, ribose 6-phosphate; 6PG, 6-phosphate gluconate; Phe, phenylalanine; 3PG, 3-phosphoglycerate; Cit, citrate; G3P, glyceraldehyde 3-phosphate; MethCoA, methylmalmonyl-CoA; S7P, sedoheptulose 6-phosphate; Leu, leucine; Tyr, tyrosine; Asn, asparagine; Gly, glycine; Ser, serine; Pro, proline; ProCoA, propionyl-CoA; Ala, alanine; Val, valine Thr, threonine; Ile, isoleucine; Met, methionine; Asp, aspartate

times as high as the control, respectively. Thus, it could be inferred that the AdpA might upregulate the genes involved in Propionyl-CoA and Methylmalonyl-CoA biosynthesis, which was identified later by transcriptional analysis of *methB* responsible for biosynthesis of Methylmalonyl-CoA.

Transcriptional analysis based on *Streptomyces* ZYJ-6 and the mutant *Streptomyces* ZYJ-6 pFAdpA

The genome of *Streptomyces* FR-008 has been completely sequenced in 2016 [24]. Generally, the genes required for antibiotic biosynthesis are clustered and co-regulated [25]. In *Streptomyces* ZYJ-6, the biosynthetic gene cluster of polyene antibiotic FR-008 (candicidin) consists of 21 genes (Fig. 4), including *pabAB* and *pabC* encoding ADC synthase and lyase, which are responsible for the biosynthesis of starter unit PABA; *fscA–fscF* encoding the type I polyketide synthase subunits constituting 21 modules; *fscTE* encoding the type II thioesterase for removing aberrant intermediates; *fscR1–fscR4* encoding four transcriptional regulators; *fscM1– fscM3* responsible for the biosynthesis of mycosamine and so on [26]. Moreover, *skaK* and *methB* were also taken into account due to their deduced functions of the biosynthesis of shikimic acid and Methylmalonyl-CoA, since shikimic acid and Methylmalonyl-CoA were important precursors of the candicidin biosynthesis (Fig. 3).

As the mutant had positive effect on the candicidin production, it was hypothesized that some genes in candicidin biosynthetic gene cluster would be regulated by *adpA*. Therefore, qRT-PCR verification was conducted to further explore the possible target genes.

The fold changes of these relative genes by qRT-PCR were calculated by the method of $2^{-\Delta\Delta CT.}$ As shown in Fig. 5, firstly, the transcription level of *adpA* exhibited obvious advantage (fold change = 22.14 >> 2) in the mutant after 46 h, demonstrating that the pleiotropic regulator *adpA* was transcribed successfully in the mutant. Under same culture conditions, the big difference in candicidin production

between the control and mutant was likely to be caused by the expression of *adpA*. The transcription of *adpA* in the mutant started at 46 h which coincided with the literature reported that the concentration of A-factor (2-isocaproyl-3-R-hydroxymethyl-g-butyrolactone) needs to reach certain threshold to trigger both secondary metabolism and morphological differentiation [27]. In this study, 46 h was the possible key point for the accumulation of A-factor. Therefore, to explore the regulatory mechanism of *adpA*, 46 h, 96 h and 156 h should be brought to the forefront.

As a result, the pleiotropic regulator *adpA* was not only transcribed successfully but also brought differential expressions of series of genes involved in candicidin biosynthesis. This study focused on the gene cluster of candicidin production and several genes encoding precursor biosynthesis.

As shown in Fig. 5, the fold change of the gene *methB* encoding biosynthesis of Methylmalonyl-CoA was improved by 7.09-fold in the mutant strain compared to the control strain. It was suggested that the gene expression of *methB* was significantly up-regulated by the presence of *adpA*. The result reconfirmed that Methylmalonyl-CoA played a vital role in the candicidin production due to the increased gene expression of *methB* as well as the metabolic flux and concentration of Methylmalonyl-CoA (Fig. 3, Table 3). In the whole process, no significant expression difference (0.5 < fold change < 2) of *skaK* was observed, indicating that the biosynthesis of shikimic acid, the first step of shikimic acid metabolism (Fig. 3), was not the bottleneck for the candicidin production in the control strain.

Particularly, in the mutant strain, the fold changes of the genes *pabAB*, *pabC* and *fscA* involved in the biosynthesis and loading of PABA, the first unit of the candicidin production (Table 1), were 1.96-, 2.31- and 3.84-fold higher than that in the control strain (Fig. 5). Except for the fold change of *pabAB* was less than two, other fold changes were more than two, suggesting that the genes *pabAB*, *pabC* and *fscA* involved in the biosynthesis and loading of PABA were strongly activated by *adpA*. Meanwhile, the concentration of PABA was almost same between the control and mutant strains (Table 3, Fig. 3). Although the correlative genes were strongly activated, the metabolic fluxes of PABA were 76.9 and 82.3 in the control and mutant, respectively. As a result, PABA was not the primary reason for the discrepancy between the control and mutant strain which is consistent with the result of metabolomics analysis.

The fold changes of the genes *fscB–fscF* and *fscTE*, which were mainly responsible for the carbon chain elongation of the candicidin (Table 1) in the mutant strain were about 5.32-, 5.77-, 5.51-, 1.59-, 1.63- and 2.08-fold improvement on the basis of that in the control strain. The fold changes were greater than two (except *fscE* and *fscF* were greater than 1.5), implying that *adpA* upregulated all the genes after the onset of the candicidin production (Fig. 4). This result
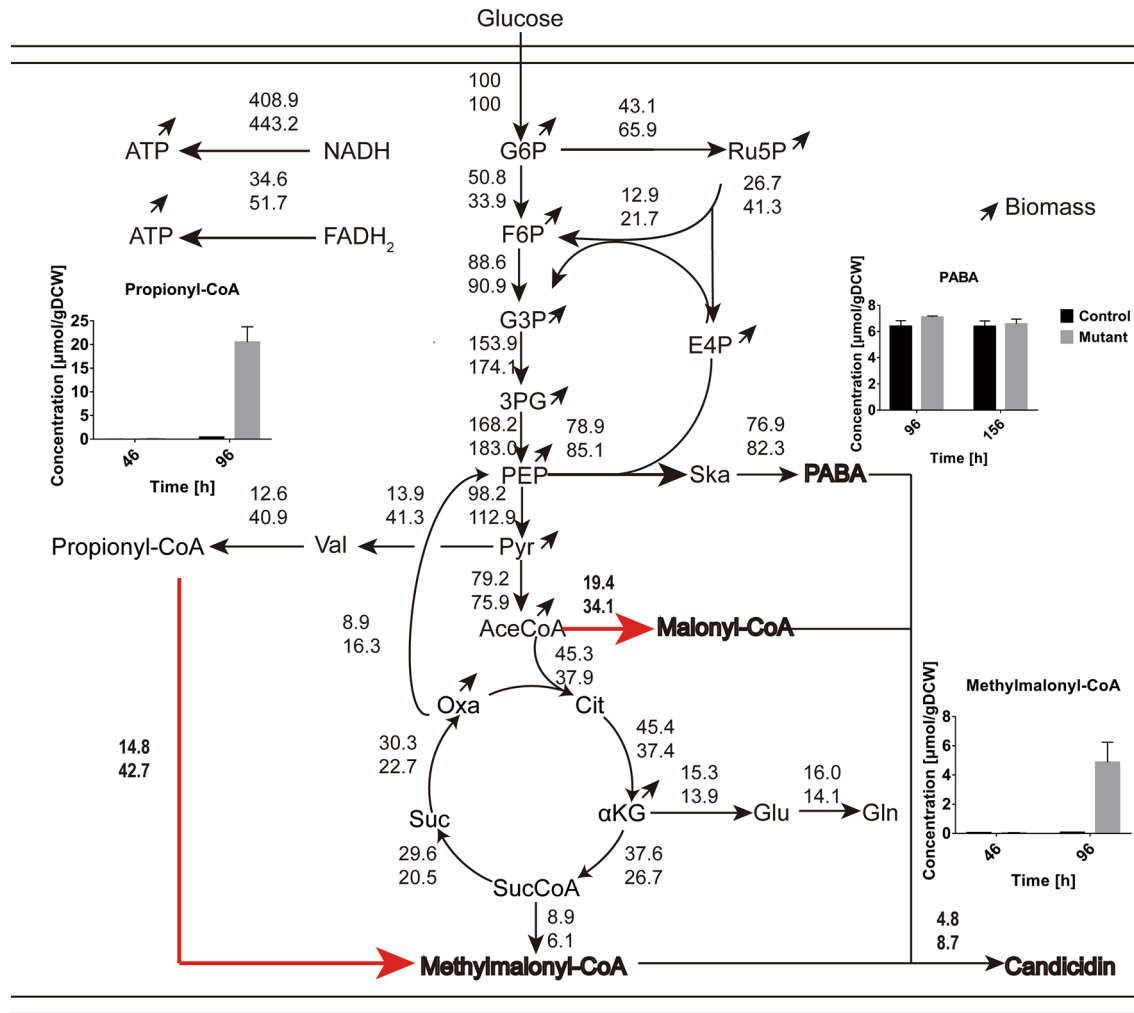
Fig. 3 The relative flux (mmol/100 mmol glucose) of the Control (*Streptomyces* ZYJ-6, upper) and Mutant (*Streptomyces* ZYJ-6 pFAdpA, lower) from 46 to 96 h. The reactions and coefficient matrix can be found in supplementary files (Tables S1, S2). The histograms of propionyl-CoA, methylmalonyl-CoA and PABA were presented here. The black column was from the control and grey column was from the mutant. G6P, glucose 6-phosphate; F6P, fructose 6-phos-phate; G3P, glyceraldehyde 3-phosphate; 3PG, 3-phospho-glycerate; PEP, phosphoenolpyruvate; Pyr, pyruvate; AceCoA, acetyl-CoA; Cit, citrate; αKG, α-ketoglutarate; Glu, glutamate; Gln, glutamine; Suc-CoA, succinyl-CoA; Suc, succinate; Oxa, oxaloacetate; Val, valine; Ru5P, ribulose 5-phosphate; E4P, erythrose 4-phosphate; Ska, shikimic acid; PABA, *para*-aminobenzoic acid
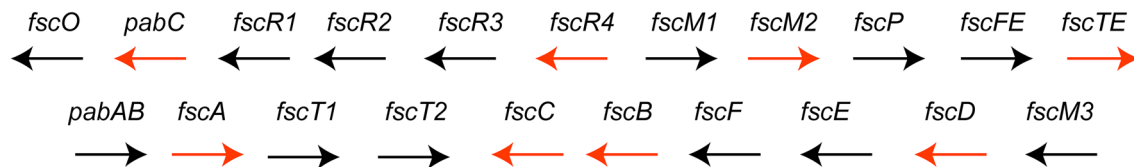
Fig. 4 The gene cluster of candicidin biosynthesis. The red arrows mean relevant genes were strongly upregulated (fold change > 2) by *adpA* in *Streptomyces* ZYJ-6 pFAdpA (Mutant) at 96 h

could account for the difference of the candicidin production between the control and mutant strains. *fscM2* and *fscM3* were responsible for the biosynthesis of mycosamine (part of the candicidin) (Table 1). In the mutant, their fold changes were 3.86- and 1.4-fold over the control strain, suggesting that *adpA* upregulated *fscM2* and *fscM3*, which were helpful for the candicidin production. *fscR3* and *fscR4* encoded transcriptional regulators and regulated the candicidin
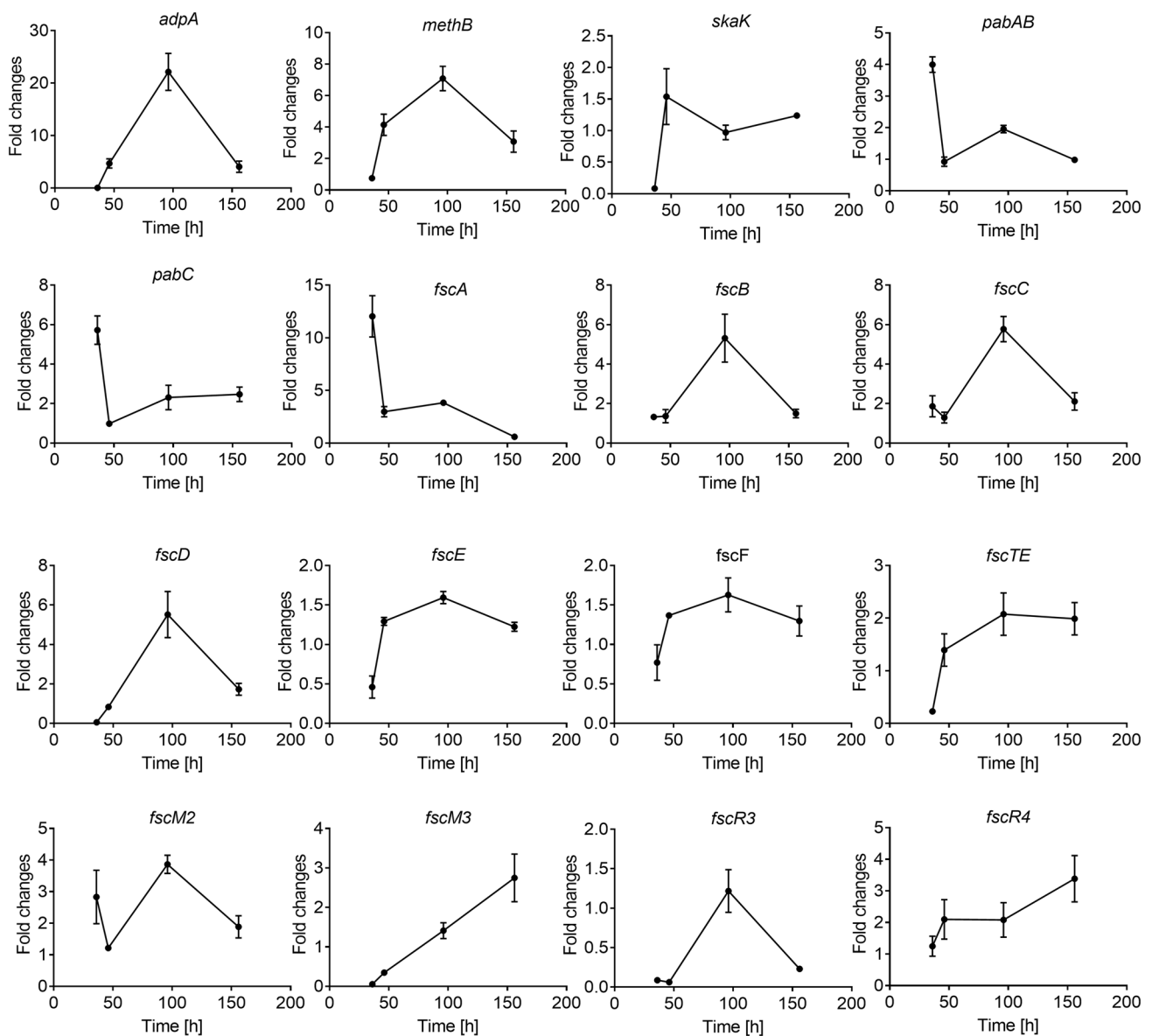
Fig. 5 Transcriptional levels of key genes between the control and mutant strain. Each value represents the average of three independent experiments and the error bars represent standard deviations

production (Table 1). In this study, the fold changes of the genes *fscR3* and *fscR4* in the mutant were 1.22- and 2.08-fold of those in the control strain. The activation had no significant differences, meaning that the regulation was not the main reason for the discrepancy of the candicidin production.

Altogether, by the analysis of transcriptional levels, the pleiotropic regulator *adpA* was introduced into the mutant strain and transcribed successfully and caused the differential expression of many genes involved in candicidin biosynthesis, especially *methB* which is responsible for Methylmalonyl-CoA synthesis. This was the direct evidence from transcriptional levels on the big difference in candicidin production between

the control and mutant. However, the shikimic acid pathway and PABA were not the primary limiting factor for the candicidin production during the early phase (46–96 h). Moreover, *fscA–fscD*, *fscTE*, *fscM2* and *methB* involved in the biosynthesis of candicidin and its precursor, were significantly upregulated by the presence of *adpA* after 46 h (Fig. 4), which might result in the increased candicidin production in the mutant.

Flux balance analysis between the control and mutant strain

Based on the analyses of metabolomics and transcriptional levels, some conclusions were drawn. However, the pool

sizes and fold changes were relatively static description. To verify the reliability of the conclusions, the metabolic flux distributions were investigated (Fig. 3).

First, the flux from Propionyl-CoA to Methylmalonyl-CoA was nearly three times (42.7/14.8) higher in the mutant than in the control (Fig. 3). In metabolomics analysis, the pool sizes of Propionyl-CoA and Methylmalonyl-CoA were 513 and 70 times in the mutant than in the control (Table 3). In transcriptional level analysis, the *methB* was upregulated significantly. All these results indicated that although the two strains were cultivated in same condition, the *adpA* resulted in the upregulation of the gene *methB* responsible for biosynthesis of Methylmalonyl-CoA and afterwards the flux of the reaction was enhanced and the pool size of Methylmalonyl-CoA showed big difference and finally, the titer of candicidin was varied considerably from 46 to 96 h. The *methB* gene might be the candidate gene target for further improving the production of candicidin.

Besides, the flux for biosynthesis of PABA was very close (82.3/76.9) in the mutant and control (Fig. 3). In the metabolomics analysis, pool sizes of PABA were barely changed in the mutant and control (Table 3, Fig. 3). In transcriptional analyses, the genes *pabAB*, *pabC* and *fscA* responsible for the biosynthesis and utilization of PABA were upregulated after 96 h and the expression level of *skaK* encoding the shikimate kinase was nearly unchanged, indicating that PABA and the first step of shikimic acid metabolism (Fig. 3) were not the bottleneck for the candicidin production in the control.

In summary, the highest level 9338 µg/mL of candicidin production was ever reported. Based on the combined analyses of transcriptional levels, metabolic flux and metabolomics, it was explained how did the pleiotropic regulator AdpA enhance the candicidin production and cell growth and found methylmalonyl-CoA played important role in candicidin production.

Conclusions

Under the same culture condition, the mutant strain was more favorable to enhancing the candicidin production and cell growth. Due to the introduction of *adpA*, the expression of some genes (*fscA–fscD*, *fscTE*, *fscM2* and *methB*) involved in candicidin biosynthesis was up-regulated greatly and enhanced the candicidin production to the titer of 9338 µg/mL, which is the highest candicidin level ever reported in the literature. Besides, *para*-aminobenzoic acid and the first step of shikimic acid metabolism were not the bottleneck and methylmalonyl-CoA played a central role in the candicidin production in the presence of *adpA*.

Compliance with ethical standards

Conflict of interest The authors declare no conflicts of interest.

References

1. Waksman SA, Reilly HC, Harris DA (1948) *Streptomyces griseus* (Krainsky) Waksman and Henrici. J Bacteriol 56(3):259–269
2. Waksman SA, Lechevalier HA, Schaffner CP (1965) Candicidin and other polyenic antifungal antibiotics: a review*. Bull World Health Organ 33(2):219–226
3. Liang RF, Zhou Q (1987) Studies on fusion breeding of protoplasta from antibiotic producing strain 5120-III. genetic analysis of fusion products. Chin J Biotechnol 3(2):130–136
4. Chen S, Huang X, Zhou XF, Bai LQ, He J, Jeong KJ, Lee SY, Deng ZX (2003) Organizational and mutational analysis of a complete FR-008/candicidin gene cluster encoding a structurally related polyene complex. Chem Biol 10(11):1065–1076
5. Liu CM, McDaniel L, Schaffner C (1975) Factors affecting the production of candicidin. Antimicrob Agents Ch 7(2):196–202
6. Zhou YJ, Li JL, Zhu J, Chen S, Bai LQ, Zhou XF, Wu HM, Deng ZX (2008) Incomplete beta-ketone processing as a mechanism for polyene structural variation in the FR-008/candicidin complex. Chem Biol 15(6):629–638. https://doi.org/10.1016/j.chembiol.2008.05.007
7. Khokhlov AS, Tovarova II, Borisova LN, Pliner SA, Shevchenko LN, Eia K, Ivkina NS, Rapoport IA (1967) The A-factor, responsible for streptomycin biosynthesis by mutant strains of *Actinomyces streptomycini*. Doklady Akademii Nauk Sssr 177(1):232–235
8. Ohnishi Y, Yamazaki H, Kato JY, Tomono A, Horinouchi S (2005) AdpA, a central transcriptional regulator in the A-factor regulatory cascade that leads to morphological development and secondary metabolism in *Streptomyces griseus*. Biosci Biotech Bioch 69(3):431–439
9. Ohnishi Y, Kameyama S, Onaka H, Horinouchi S (1999) The A-factor regulatory cascade leading to streptomycin biosynthesis in *Streptomyces griseus*: identification of a target gene of the A-factor receptor. Mol Microbiol 34(1):102–111
10. Guyet A, Benaroudj N, Proux C, Gominet M, Coppée JY, Mazodier P (2014) Identified members of the *Streptomyces lividans* AdpA regulon involved in differentiation and secondary metabolism. BMC Microbiol 14(1):1–12
11. Tan GY, Peng Y, Lu CY, Bai LQ, Zhong JJ (2015) Engineering validamycin production by tandem deletion of gamma-butyrolactone receptor genes in *Streptomyces hygroscopicus* 5008. Metab Eng 28:74–81
12. Zhao JL, Ying C, Song Y, Ji L (2007) An *adpA* homologue in *Streptomyces avermitilis* is involved in regulation of morphogenesis and melanogenesis. Chin Sci Bull 52(5):623–630
13. Nguyen KT, Tenor J, Stettler H, Nguyen LT, Nguyen LD, Thompson CJ (2003) Colonial differentiation in *Streptomyces coelicolor* depends on translation of a specific codon within the *adpA* Gene. J Bacteriol 29(5):75–98
14. Wang T, Bai LQ, Zhu DQ, Lei X, Liu G, Deng ZX, You DL (2012) Enhancing macrolide production in *Streptomyces* by

coexpressing three heterologous genes. Enzyme Microb Tech 50(1):5–9

15. Mao XZ, Shen YL, Wei DZ, Chen S, Deng ZX (2005) Determination of candicidin/FR-008 and related components in fermentation broth by RP-HPLC. J Chin Pharmaceutical Sci 14(2):115–118

16. de Jonge LP, Buijs NA, ten Pierick A, Deshmukh A, Zhao Z, Kiel JA, Heijnen JJ, van Gulik WM (2011) Scale-down of penicillin production in penicillium chrysogenum. Biotechnol J 6(8):944–958

17. Cipollina C, ten Pierick A, Canelas AB, Seifar RM, van Maris AJA, van Dam JC, Heijnen JJ (2009) A comprehensive method for the quantification of the non-oxidative pentose phosphate pathway intermediates in *Saccharomyces cerevisiae* by GC-IDMS. J Chromatogr B 877(27):3231–3236

18. Hong M, Mou H, Liu X, Huang M, Chu J (2017) ^{13}C-assisted metabolomics analysis reveals the positive correlation between specific erythromycin production rate and intracellular propionyl-CoA pool size in *Saccharopolyspora erythraea*. Bioproc Biosyst Eng 40:1337–1347. https://doi.org/10.1007/s00449-017-1792-0

19. Zhang P, Zhao Z, Li H, Chen X-L, Deng Z, Bai L, Pang X (2015) Production of the antibiotic FR-008/candicidin in *Streptomyces sp.* FR-008 is co-regulated by two regulators, FscRI and FscRIV, from different transcription factor families. Microbiol 161(Pt 3):539–552. https://doi.org/10.1099/mic.0.000033

20. Livak KJ, Schmittgen TD (2001) Analysis of relative gene expression data using real-time quantitative PCR and the 2(-Delta Delta C(T)) Method. Methods 25(4):402–408

21. Chen Y, Huang M, Wang Z, Chu J, Zhuang Y, Zhang S (2013) Controlling the feed rate of glucose and propanol for the enhancement of erythromycin production and exploration of propanol metabolism fate by quantitative metabolic flux analysis. Bioprocess Biosyst Eng 36(10):1445–1453

22. Guyet A, Benaroudj N, Proux C, Gominet M, Coppee JY, Mazodier P (2014) Identified members of the *Streptomyces lividans* AdpA regulon involved in differentiation and secondary metabolism. BMC Microbiol 14:81. https://doi.org/10.1186/1471-2180-14-81

23. Tang L, Zhang YX, Hutchinson CR (1994) Amino acid catabolism and antibiotic synthesis: valine is a source of precursors for macrolide biosynthesis in *Streptomyces ambofaciens* and *Streptomyces fradiae*. J Bacteriol 176(19):6107–6119

24. Liu Q, Xiao L, Zhou Y, Deng K, Tan G, Han Y, Liu X, Deng Z, Liu T (2016) Development of *Streptomyces sp.* FR-008 as an emerging chassis. Synth Syst Biotechnol 1(3):207–214

25. Horinouchi S (2007) Mining and polishing of the treasure trove in the bacterial genus *Streptomyces*. Biosci Biotech Bioch 71(2):283–299

26. Zhang YR, Bai LQ, Deng ZX (2009) Functional characterization of the first two actinomycete 4-amino-4-deoxychorismate lyase genes. Microbiol Sgm 155:2450–2459. https://doi.org/10.1099/Mic.0.026336-0

27. Higo A, Hara H, Horinouchi S, Ohnishi Y (2012) Genome-wide distribution of AdpA, a global regulator for secondary metabolism and morphological differentiation in *Streptomyces*, revealed the extent and complexity of the AdpA regulatory network. Dna Res An Int J Rapid Publ Rep Genes Genomes 19(3):259–274